

Self-similarity in a system with a short-time delayed feedback

Liu Yaowen,^{*} Li Haibin, Zhao Hong,[†] Wang Yinghai[‡]

Department of Physics, Lanzhou University, Lanzhou 730000, China

(October 1, 2018)

Using the Poincaré section technique, we study in detail the dynamical behaviors of delay differential system and find a new type of solutions S_i in short-time delay feedback. Our numerical results remind us to deny the opinion that there are no complex phenomena in short-time delay case. Many similarities between fundamental solution and the new type of solutions are found. We demonstrate that the scales of S_i increase with exponential growth via i in the direction of μ , while decrease with exponential decays in the direction of x or delay time t_R .

I. INTRODUCTION

Optical feedback systems governed by delay differential equations (DDEs) have attracted much attention from both the applied and the fundamental points of view [1-16]. Generally, the delay-differential system related to optical bistable or hybrid optical bistable device is described by

$$\tau' \dot{x}(t) = -x(t) + f(x(t - t_R), \mu), \quad (1)$$

where $x(t)$ is the dimensionless output of the system at time t , t_R is the time delay of the feedback loop, τ' is the response time of the nonlinear medium, the parameter μ is proportional to the intensity of the incident light. In Eq. (1), $f(x, \mu)$ is a nonlinear function of x , characterizing the system, e.g. $f(x, \mu) = \mu\pi[1 - \zeta \cos(x - x_B)]$ for Ikeda model [2], $f(x, \mu) = \pi[A - \mu \sin^2(x - x_0)]$ for Vallée model [3], and $f(x, \mu) = \mu \sin^2(x - x_0)$ for the sine-square model [4].

The understanding of the Eq. (1) up to now can be summarized as follows. The first experimental observation of period-doubling bifurcations and chaos in a hybrid bistable device was made by Gibbs *et al.* [1] following a prediction by Ikeda *et al.* [2]. The solution of system, which appears after Hopf bifurcation, evolves through a period doubling $T_F \rightarrow 2T_F \cdots \rightarrow 2^N T_F$, as one parameter is varied. These solutions are called 2^N periodic and the cascade accumulates at the Feigenbaum point. These solutions are named *fundamental solutions* by Ikeda *et al.* [2], we do so in this paper. Later the two groups found that *higher-harmonic* oscillation states appear successively in the course of transition to developed chaos in long-time delayed case (i.e. delay time is longer enough than the response time). These solutions coexist and each follows a period-doubling cascade. The oscillation period of these harmonic states are given by T_F/n , where n is odd integer and T_F is the period of the fundamental solution. As the study of the dimension of the chaotic attractor, the behavior of the DDE exhibits high-dimensional chaos [5]. Ikeda and Matsumoto have given an estimate of the Lyapunov dimension of attractor for the Ikeda model, and it ranges approximately from 2 to 13 when some bifurcation parameter is varied. Recently, some researchers demonstrated that the behavior of quasiperiodicity followed the hierarchy of the Farey tree [6–10] and the chaotic itinerancy phenomenon switches among some different unstable local chaotic orbits [11–13]. We reported two new types of solutions found in moderate-time and short-time delay regimes [15], which are different from *the fundamental solution* and *the odd harmonic solution*. In this paper, we study in detail the dynamical behaviors of the new type of solution found in short-time delay regimes.

This paper is organized as follows: In Sec. II, the numerical methods used in this paper are introduced. By using Poincaré section technique, we can easily observe the course of bifurcation of DDE, and easily distinguish the new type of solutions and the fundamental solution. In Sec. III, we demonstrate our numerical results. In the short-time delay case, there is a new type of solutions $S_i (i = 1, 2, 3, \dots)$, which has many similarities comparing with fundamental solution. Moreover, these new solutions are alike each other. In Sec. IV we summarize our results and conclude.

^{*}E-mail address: chaosun@lzu.edu.cn

[†]E-mail address: zhaoh@lzu.edu.cn

[‡]Author to whom correspondence should be addressed. E-mail: wangyh@lzu.edu.cn

II. NUMERICAL METHODS

Measuring the delay time in units of t_R , one can rewrite Eq. (1) as

$$\tau \dot{x}(t) = -x(t) + f(x(t-1), \mu), \quad (2)$$

where $\tau = \tau'/t_R$ characterizes the effect of the time delay when τ' is fixed. In this paper, we study Eq.(2) with the special feedback function

$$f(x, \mu) = 1 - \mu x^2. \quad (3)$$

This feedback function can be considered as the first nonlinear term of the Taylor expansion of the general nonlinear function $f(x, \mu)$ in the vicinity of a steady state. It should keep the general nonlinear properties of DDE, as shown in Refs. [14,15].

The Eq. (2) can be solved numerically and a fourth-order Adam's interpolation is suitable for that. In order to trace the evolution of a DDE, one might investigate the evolution curve of the variable $x(t)$ vs the time t . However, it is difficult to distinguish different solutions if one only observes the $x(t) - t$ relation. Some of us (Zhao *et al.*) have offered a method in Ref. [10] to represent the solutions of a one-variable DDE by using the Poincaré section technique. This method has been proved to be a powerful tool in exploring the evolution of bifurcation of DDE. Let us review this method briefly. Let $x_i(\theta) \equiv x(t+\theta)$, $-1 \leq \theta \leq 0$, then $x_{t_2}(\theta)$ is determined by $x_{t_1}(\theta)$ uniquely according to Eq. (2), where $t_1 < t_2$. We approach the section mapping as follows: choose an appropriate constant $x_c \in R$; integrate Eq. (2) numerically till $x(t) > x_c$ and $x(t+h) < x_c$, where h is the length of the integrating step; then proceed a simulation procedure to get t_i as well as $x_{t_i}(\theta)$ such that $x_{t_i}(0) = x_c$. To be simple, we denote $x_{t_i}(\theta)$ as $x_i(\theta)$ in the following discussions. In this way we convert the flow of Eq. (2) into a mapping which maps the curve $x_i(\theta)$ onto the curve $x_{i+1}(\theta)$. We regard this curve-to-curve mapping as the Poincaré map of a DDE. A periodic solution of Eq. (2) with period T , $x(t) = x(t+T)$, corresponds to a periodic solution of the Poincaré map with period N , $x_i(\theta) = x_{i+N}(\theta)$, where N is an integer. For practical applications, we can take n discrete points $x_i(\theta_j)$ on the curve $x_i(\theta)$ to represent the solution, where $\theta_j \in (-1, 0)$ and $j = 1, 2, \dots, n$. Then the curve-to-curve mapping appears as a point-to-point mapping in R^n . In order to exhibit the bifurcation process, here we usually need a one-dimensional mapping representation $x_i(\theta_1)$ with the bifurcation parameter.

III. RESULTS

As usually considered, there is no complex phenomenon in short-time delay region since Eq. (2) will approach a normal one-dimensional ordinary differential equation. Our results remind us that this is not the truth.

A. The bifurcation of fundamental solution

Before discussing the new type of solutions, let us first review the bifurcation process of the fundamental solution. In the long-time delay case (i.e. τ is very small), Ikeda *et al.* [2] have shown theoretically that instabilities and chaotic behaviors can occur in the system. As τ is fixed and μ is increased, a square-wave solution appears after the Hopf bifurcation of a steady state. With further increase of μ , this square wave solution undergoes a square of bifurcation with its period doubling itself successively and then becomes chaotic. We define this solution as *the fundamental solution* of the system and marked it as S_0 .

When τ increases (i.e. delay time decreases), the fundamental solution exhibits mirror-similar bifurcation behavior as shown in Fig. 1(a). With the continuous increase of τ , the period-doubling bifurcation with less and less order takes place in the course of bifurcation. At $\tau = 1.13$, S_0 undergoes only period-two bifurcation via μ . Fig.1(b) shows a bifurcation diagram just below this value. With further increase τ , we can no longer observe the period-doubling bifurcation of S_0 , see Fig. 1(c)-(f). We regard the regime of $\tau > 1.13$ as short-time delay case. In this regime, the delay time t_R is smaller than the response time τ' because $\tau = \tau'/t_R$, and the fundamental solution exhibits only one-period limit cycle state.

B. New type of solutions

In the short-time delay case, fundamental solution shows no bifurcation and chaos. This is not to say that there is no chaos in this system with the varying of μ at a fixed parameter τ . In fact, there still exists another chaotic attractor,

which locates behind S_0 in the direction of μ , as shown in Fig. 1(c)-(f). We marked them as $S_i (i = 1, 2, 3, \dots)$. In the direction of μ , every S_i evolves a period-doubling bifurcation. Figure 2 exhibits the evolution courses of fundamental solution and S_i , which is located on period-one limit cycle state of themselves, respectively.

From Fig. 1 and Fig. 2, we can easily find that there are not only similarities but also difference among S_0 and S_i . Firstly, with the increase of τ , each S_i appears the same bifurcation process as S_0 does. Comparing Fig. 1(c) with Fig. 1(a), we can find the diagram of S_1 at $\tau = 3.0$, displays the same shape as that of S_0 at $\tau = 0.80$. In fact, at certain parameter, S_2, S_3 and S_4 *et al.* also show the similar shape. Secondly, S_i has more and more oscillation with the increase of the subscript i . Simultaneously, i increases with the increase of τ . S_0 has only one peak within one period. In contrast to S_0 , S_1 has not only the peak but also another small peak; S_2, S_3 and S_4 have more and more peaks within one period respectively, see Fig. 2. Thirdly, with the increase of τ , S_i appears one by one and S_1 follows S_0 , S_2 follows S_1 in the direction of μ .

C. The scales of S_i via i

From Fig. 1 one can find that S_i appears continually with the increase of τ . In order to find the law which exhibits the appearance order of S_i and the scales of S_i , we should choose a standard to compare S_i with each other. In this paper, we choose the critical values of τ_i as the standard, τ_i is the value at which the second period-doubling bifurcation of the period-1 solution of S_i takes place with the decrease of τ . In fact one could also choose another standard. For this specific choice, the bifurcation diagram of S_i appears as the patterns in Fig. 3(a)-(e) respectively. Our numerical solutions show that τ_i increases with exponential growth against the increase of i . Figure 4(a) demonstrates the result, where the scatters are the values of τ_i and the dotted line is the fitting curve which is exponential growth function with the increase of i as follows: $\tau_i = A \exp(i/B)$, where A and B are fitting coefficients..

From Fig. 1 one can find the scale of the bifurcation diagrams of S_i along μ increases, while along x decreases with the increase of i . Using the standard chosen above, we can measure the length $\delta\mu$ of the period-2 solution in the direction of μ at τ_i and use it to characterize the scale of S_k along μ . Figure 4(c) shows that $\delta\mu$ also increases with exponential growth via i , and the exponential function is $\delta\mu(i) = A \exp(i/B)$. On the other hand, by measuring the maximum height δx of the period-2 solution at τ_i , we find that δx exhibits the exponential decay with the increase of i : $\delta x(i) = A \exp(-i/B)$, see Fig. 4(d).

IV. CONCLUSION

In this paper we have studied in detail the dynamics of short-time delay differential system. Our numerical result remind us that it is not truth to consider that there is no complex behavior in short-time delay feedback. By using the Poincaré section technique in DDE [10], a new type of solutions S_i was found in this case and it has many similarities as same as fundamental solution in the bifurcation diagrams. We found the law of S_i and showed the scales of S_i with the increase of i . The scales of S_i increases along μ and τ , while decreases along x and delay time .

ACKNOWLEDGMENT

This work is supported in part by the National Natural Science Foundation of China, and in part by Doctoral Education Foundation of National Education Committee.

-
- [1] H.M. Gibbs, F.A. Hopf, D.L. Kaplan, and R.L. Shoemaker, Phys. Rev. Lett. **46** (1981) 474; Phys. Rev. A **25** (1982) 2172.
 - [2] K. Ikeda, H. Daido, O. Akimoto, Phys. Rev. Lett. **45** (1980) 709; Phys. Rev. Lett. **49** (1982) 1467.
 - [3] R. Vallée, C. Delisle, Phys. Rev. A **34** (1986) 309.
 - [4] J.P. Goedgebuier, L. Larger, and H. Porte, Phys. Rev. E **57** (1998) 2795.
 - [5] B. Dorizzi, B. Grammaticos, M. Le Berre, Y. Pomeau, E. Ressayre, and A. Tallet, Phys. Rev. A **35** (1987) 328 ; K. Ikeda and K. Matsumoto, Physica 29D (1987) 223.
 - [6] D. Baums, W. Elsässer, and E. O. Göbel, Phys. Rev. Lett. **63** (1989) 155.
 - [7] J. Mørk, J. Mark, and B. Tromborg, Phys. Rev. Lett. **65** (1990) 1999.
 - [8] J. Sacher, D. Baums, P. Panknin, and E. O. Göbel, Phys. Rev. A **45** (1992) 1893.

- [9] J. Ye, H. Li, and J. G. McInerney, Phys. Rev. A **47** (1993) 2249.
- [10] H. Zhao, F. Z. Zhang, J. Yan, and Y. H. Wang, Phys. Rev. E **54** (1996) 6925.
- [11] K. Otsuka, Phys. Rev. Lett. **65** (1990) 329.
- [12] I. Fischer, O. Hess, W. Elsässer, and E. Göbel, Phys. Rev. Lett. **73** (1994) 2188.
- [13] C. Masoller, Phys. Rev. A **50** (1994) 2569.
- [14] J. N. Li and B. L. Hao, Commun. Theor. Phys. **11** (1989) 265.
- [15] H. Zhao, Y.W. Liu, Y.H. Wang, and B.B Hu, Phys. Rev. E **58** (1998) 4383.
- [16] A.R. Volkovskii and N.F. Rulkov, Tech. Phys. Lett. **19** (1993) 97.

FIG. 1. The bifurcation diagrams of S_0 and S_i with the increase of τ .

FIG. 2. The evolution of S_0 and S_i versus time. (a) $S_0, \tau = 0.3, \mu = 1.50$; (b) $S_1, \tau = 1.5, \mu = 8.50$; (c) $S_2, \tau = 1.5, \mu = 9.42$; (d) $S_3, \tau = 3.5, \mu = 31.45$; (e) $S_4, \tau = 40, \mu = 2585$.

FIG. 3. Bifurcation diagrams of S_0 and S_i at the critical values of τ_i .

FIG. 4. (a) τ_i , (b) t_R , (c) $\delta\mu$, and (d) δx of S_i versus i . Here τ_i is as same as figure 3 and $t_R = \tau'/\tau$. $\delta\mu$ is the length and δx is the maximum height of period-2 solution in Fig. 3 respectively. The square scatter is the numerical result and the dotted line is the fitting curves. (a) $\tau_i = 2.026 \exp(i/0.817)$; (b) $t_R(i) = 1.135 \exp(-i/0.747)$; (c) $\delta\mu(i) = 1.072 \exp(i/0.616)$; (d) $\delta x(i) = 0.125 \exp(-i/0.458)$.

Fig. 1

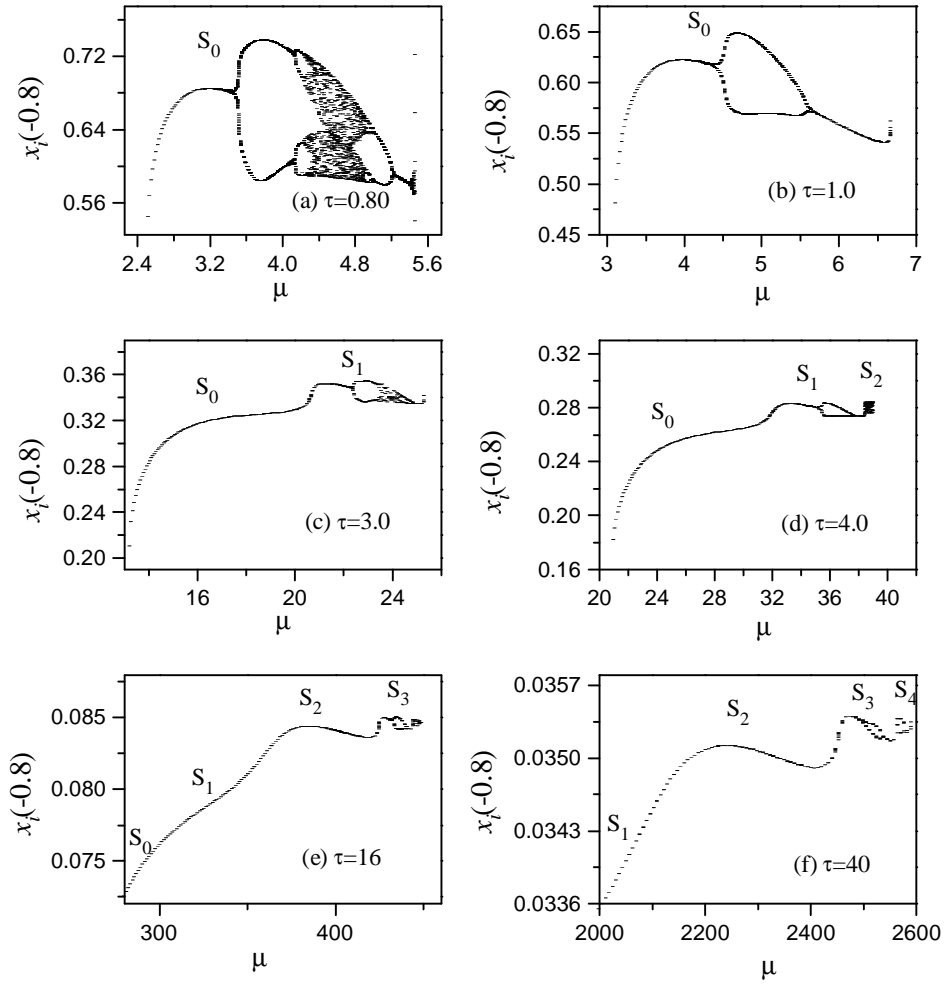


Fig. 2

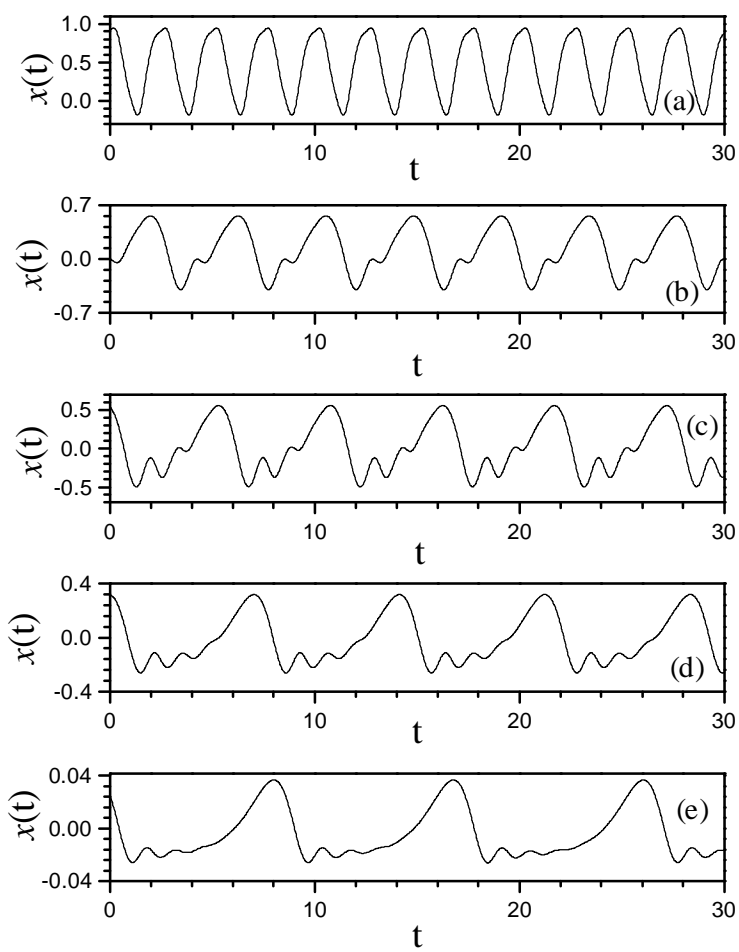


Fig.3

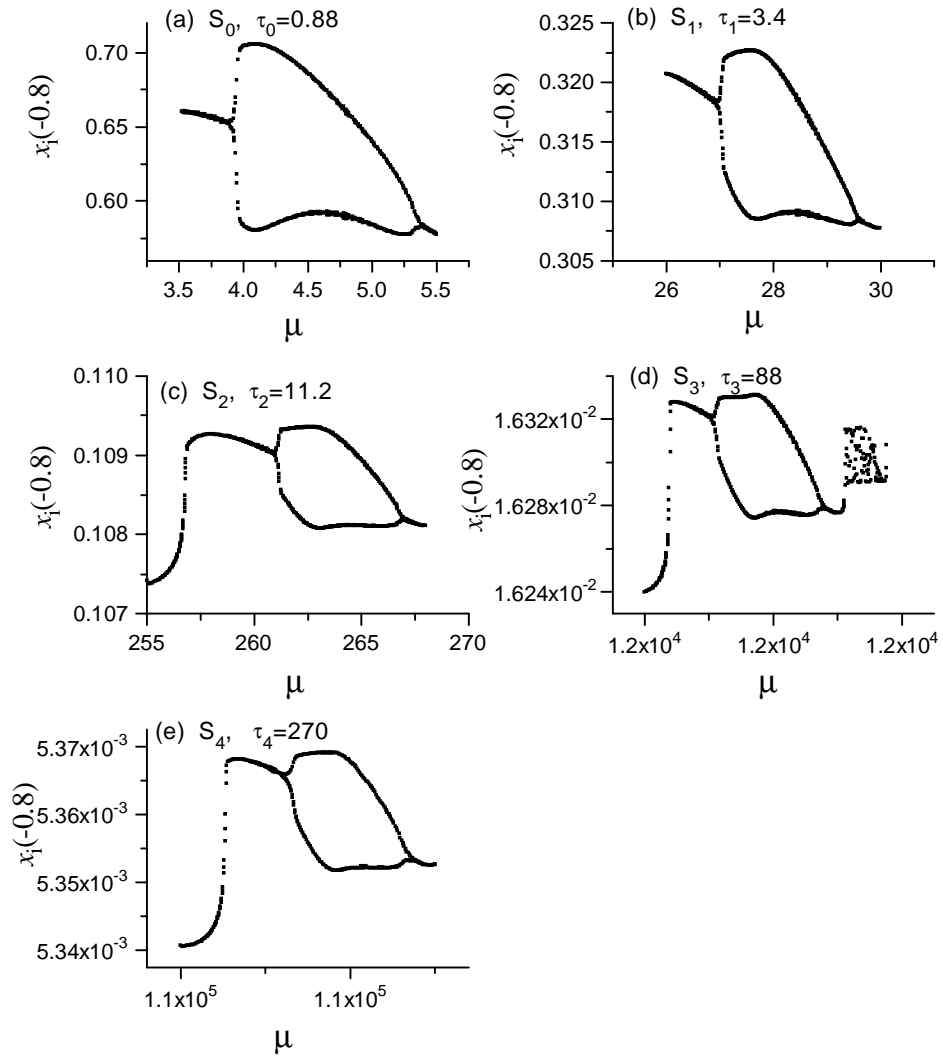


Fig. 4

